STRANGENESS AND IN-MEDIUM EFFECTS IN HEAVY ION COLLISIONS AT SIS ENERGIES

Signs for transition towards partially restored chiral symmetry ?

P. CROCHET
GSI-KP1
PLANCKstr. 1
D-64291 Darmstadt

1. Introduction

Heavy ion collisions in the beam energy range 1-2 AGeV offer interesting possibilities to study the bulk properties of hot and dense hadronic matter. Indeed, at these bombarding energies the density of the nuclear system created during the reaction is expected to reach up to three times the normal nuclear density and its temperature is of about 90 AMeV [1, 2, 3, 4]. Under such conditions the fireball consists of a composite system of strongly interacting nucleons energetic enough to give rise to resonance state excitation and meson production [5, 6, 7]. The abundance and dynamical properties of emerging particles, which have been extensively studied over the two last decades in both experimental data and theories, are recognized as useful tools to provide information about the nuclear equation of state at high densities. Beside probing the global properties of compressed hadronic matter, recent theoretical works predict that the hot and dense nuclear medium might undergo a phase transition towards partially restored chiral symmetry of QCD, leading to possible dropping hadron masses [8, 9]. Such a scenario has attracted much interest recently since it was succesfully used to describe the low mass dilepton enhancement observed by the CERES and HELIOS-3 collaborations at CERN SPS [10, 11]. Similar theories suggest that comparable in-medium effects should be observed at lower incident energies and not only on vector mesons but also on pseudo-scalar mesons [8]. In this respect, the study of sub-threshold or close-to-threshold kaon production (*i.e.* at SIS energies) is especially interesting since *i)* kaon being one of the so-called "Goldstone boson of spontaneously broken chiral symmetry", its properties are directly connected to chiral symmetry breaking and restoration, *ii)* because of its strange quark content, kaon carries special features as compared to other Goldstone bosons like pion, and *iii)* the sensitivity to in-medium effects is particularly pronounced for a particle species close to its production threshold. However, before to draw any solid conclusion, one needs to study as many observables as possible and to explore the whole available phase space of the reaction. Therefore, in order to provide quantitative basis for such investigations, the FOPI collaboration has measured charged kaons and neutral strange particles together with baryons in Ni + Ni and Ru + Ru collisions at 1.93 and 1.69 AGeV, respectively.

Here we review the most recent results obtained from these measurements. A brief introduction on kaon properties in dense nuclear matter is given in section 2. The FOPI detector is described in section 3. Experimental data on kaon phase space distributions and flow are presented with different model predictions in section 4 and 5, respectively. Finally, summary and outlooks are given in section 6.

2. Kaons in dense nuclear matter

Kaon properties in nuclear matter is currently a topic of great interest since they were shown to be possibly connected to a partial restoration of chiral symmetry with increasing baryonic density and/or temperature. They are also particularly relevant for the understanding of the strangeness enhancement in heavy ion collisions (which was proposed as a signature of a quark gluon plasma [12]) and of the limitation of neutron stars masses due to possible kaon condensation [13]. The first investigations in this field have been done in the framework of a non-linear chiral Lagrangian [14] and then extended with other approches (see [8] and ref. therein).
In the mean-field approximation to the effective $\mathrm{SU(3)_L} \times \mathrm{SU(3)_R}$ chiral Lagrangian, a dispersion relation for the kaon in a nuclear medium can be written as [15] :

$$\omega^2_{\mathrm{K}^\pm}(k, \rho_\mathrm{B}) = m^2_\mathrm{K} + k^2 - \frac{\Sigma_\mathrm{KN}}{f^2}\rho_\mathrm{S} \pm \frac{3}{4}\frac{\omega}{f^2}\rho_\mathrm{B} \qquad (1)$$

where m_K and k are the kaon bare mass and its momentum, respectively. The additional terms include a scalar interaction (third term) and a vector interaction (fourth term) of the kaon with the medium. Their strenght is fixed by the so-called kaon-nucleon sigma term Σ_KN, the nuclear scalar density ρ_S, the kaon decay constant f, and the nuclear density ρ_B.
The scalar interaction is attractive for kaons and anti-kaons whereas the vector interaction is attractive for anti-kaons and repulsive for kaons. From the above relation, one can write the kaon energy as :

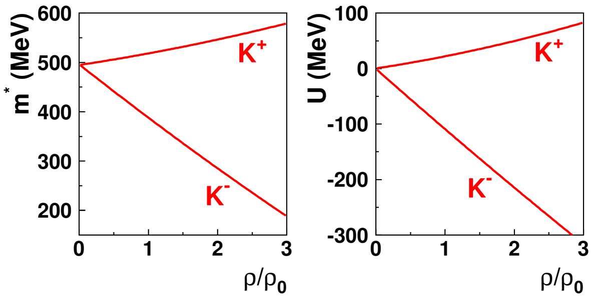

Figure 1. Kaon and anti-kaon effective mass $m^*_{\rm K}$ (left) and potential U (right) as a function of the nuclear density ρ normalised to the normal nuclear density ρ_0 (adapted from [16]).

$$\omega_{\rm K^\pm}(k,\rho_{\rm B}) = \left[m_{\rm K}^2 + k^2 - \frac{\Sigma_{\rm KN}}{f^2}\rho_{\rm S} + \left(\frac{3}{8}\frac{\Sigma_{\rm KN}}{f^2}\right)^2\right]^{\frac{1}{2}} \pm \frac{3}{8}\frac{\rho_{\rm B}}{f^2} \tag{2}$$

The effective mass $m^*_{\rm K^\pm}$ of a kaon at rest is then given by :

$$m^*_{\rm K^\pm} = \omega_{\rm K^\pm}(0,\rho_{\rm B}) \tag{3}$$

and the kaon-nucleon potential U by :

$$\mathrm{U}_{\rm K^\pm}(k,\rho_{\rm B}) = \omega_{\rm K^\pm}(k,\rho_{\rm B}) - \sqrt{m_{\rm K}^2 + k^2} \tag{4}$$

The kaon effective mass and potential are shown in Fig. 1 as a function of the nuclear density [16]. They vary differently for $\rm K^+$ and $\rm K^-$ due to the different sign in the vector interaction. The $\rm K^+$ effective mass thus slightly increases while the $\rm K^-$ effective mass is strongly reduced. Same trends were found in [17, 18, 19, 20]. Measurements of sub-threshold kaon production offer the means to test these predictions since one would expect to observe an enhanced $\rm K^-$ yield (its production being energetically much easier) and a reduced $\rm K^+$ yield (its production being energetically much difficult)[1]. On the other hand the existence of a K-nucleon potential can be tested by looking at kaon phase space distributions and/or kaon flow. Thus one would expect to observed $\rm K^+$ to be pushed away from nucleons and $\rm K^-$ to be pulled towards nucleons. First signs of such in-medium modifications of kaon properties has indeed been recently observed experimentally [21, 22].

3. Kaon identification with the FOPI detector

The FOPI detector [23] is an azimuthally symmetric apparatus made of several sub-detectors which provide charge and mass determination over nearly the full 4π solid angle. For the analysis presented here, only the Central Drift Chamber (CDC), the time of flight array (Barrel) and the forward

[1] Due to an associate production (strangeness conservation) the actual yield depends on the medium modifications of all the particles involved in one channel production.

plastic wall (PLA) were used. The latter provides in the forward part of the reactions ($1.2^\circ < \Theta_{\rm lab} < 30^\circ$) the charged particle multiplicity PMUL used for event centrality determination. The CDC and the Barrel are placed in a solenoidal magnetic field of 0.6 T. Pions, kaons, protons, deuterons and tritons are identified in the backward hemisphere ($39^\circ < \Theta_{\rm lab} < 150^\circ$) with the CDC by means of the Bethe-Bloch relation of the energy loss of a track with its momentum. This identification is improved by adding to the previous informations the particle velocity which is determined from the extrapolation of a track in the CDC to the appropriate hit in the Barrel. Kaon identification is possible only for transverse momenta above $p_{\rm t} = 0.1$ GeV/c which is needed for a particle to reach the Barrel. The upper momentum limit to which kaons can be identified without significant contamination from pions and protons is 0.5 GeV/c for K^+ and of about 0.33 GeV/c for K^- [32]. The total number of identified kaons for the two systems studied here is reported in Tab. 1.

System	Beam Energy	N(K^+)	N(K^-)
Ni + Ni	1.93 AGeV	30000	250
Ru + Ru	1.69 AGeV	40000	250

TABLE 1. Number of identified K^+ and K^- in Ni + Ni and Ru + Ru collisions at 1.93 AGeV and 1.69 AGeV, respectively.

It should be mentioned that the small statistics recorded for K^- is only partially due to the limited acceptance but rather to the production threshold for K^- (2.5 GeV) which is much higher than the one for K^+ (1.58 GeV).

4. Kaon phase space distributions

The longitudinal and transverse kaon phase space distributions are presented in this section by means of transverse mass spectra and the K^-/K^+ ratio. This is done for central events where the kaon phase space distributions is quite isotropic in the azimuthal degree of freedom [21].

4.1. TRANSVERSE MASS SPECTRA

Transverse mass spectra *i.e.* $\mathrm{d}^2\mathrm{N}/(m_{\rm t}^2 \mathrm{d}m_{\rm t}\mathrm{d}y^{(0)})$ *versus* $m_{\rm t} - m_0$ with $m_{\rm t} = (p_{\rm t}^2 - m_0^2)^{1/2}$ is nowadays commonly used to present heavy ion data beyond 1 AGeV. In the above expression m_0 is the particle rest mass and $y^{(0)}$ is the particle rapidity normalized to the projectile rapidity in the center-of-mass (c.m.) system[2]. This representation has the advantage that, in the absence

[2]With this normalization $y^{(0)} = -1, 0, 1$ correspond to target, c.m. and projectile rapidity, respectively

of flow, a thermalized system is expected to show single exponential shape in a narrow rapidity window. It can thus be parametrized with a Boltzmann-type function :

$$\frac{1}{m_t^2}\frac{\mathrm{d}^2\mathrm{N}}{\mathrm{d}m_t\mathrm{d}y^{(0)}} = A\,exp\left[\frac{-(m_t - m_0)}{\mathrm{T_B}}\right] \tag{5}$$

where A and $\mathrm{T_B}$ are parameters. $\mathrm{T_B}$ is called the Boltzmann inverse slope parameter and is interpreted as the apparent temperature of the source. This formalism has been extensively used to investigate the degree of thermal equilibrium and the amount of stopping in the systems Ni + Ni and Au + Au between 1 and 2 AGeV [5, 24, 25, 26]. We focus here on a comparison of the data for K^+ to the predictions of a transport model.

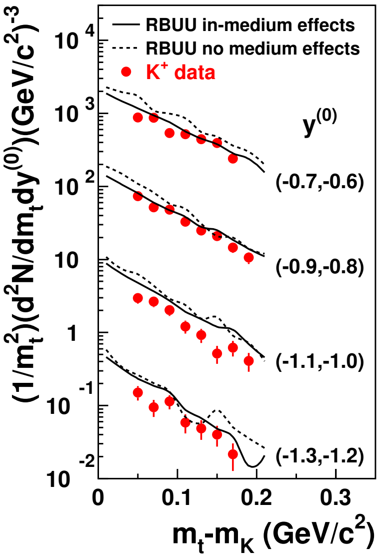

Figure 2. Transverse mass spectra of K^+ in central ($b < 4$ fm) Ru + Ru reactions at 1.69 AGeV (adapted from [27]). From the bottom to the top the spectra have been multiplied by 10^n starting with $n = 0$ for the lowest one. Data (dots) are compared to the predictions of a RBUU model [28] with in-medium effects (solid curves) and without in-medium effects (dashed curves) (see text).

Figure 2 shows transverse mass spectra of K^+ in central Ru + Ru collisions at 1.69 AGeV. The results are presented in different rapidity slices from target rapidity (bottom) to more central rapidities (top). Data are compared to the predictions of a RBUU model [28] with 2 scenarios : without and with in-medium effects. The first situation corresponds to a standard calculation including binary collisions plus all “conventional” potentials (like Coulomb potential). In the second scenario in-medium effects, as described in section 2, are included on baryons and mesons. Both sets of simulated events were first passed through the FOPI detector filter and then analyzed with the same procedure as the one used for the data.

The data points exhibit for all rapidities a single exponential behaviour thus indicating a thermal equilibrium. This trend is well reproduced by the model irrespective of the scenario considered. Indeed the sensitivity of the spectra to in-medium effects is very small.

Since the spectra are well described by single exponential functions, each of them were fitted with eq. (5) [27]. This allows to extract for each rapidity slice the apparent temperature T_B and the K^+ yield $dN/dy^{(0)}$, the latter being given by integrating the fitting function from $p_t = 0$ to ∞. These two quantities are shown in Fig. 3.

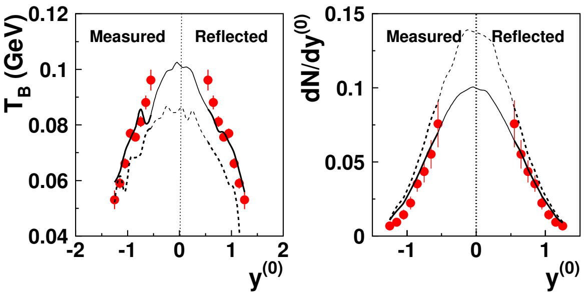

Figure 3. Apparent temperature T_B (left) and density rapidity $dN/dy^{(0)}$ (right) distributions extracted from fits to the spectra of Fig. 2 (see text). Data are mesured for negative $y^{(0)}$ and then reflected for positive $y^{(0)}$. Adapted from [27].

It is seen that in-medium effects lead to a higher T_B and a lower yield (as expected from Fig. 1). An overall better agreement with the data is observed if in-medium effects are taken into account in the calculation. However, in the rapidity range where a comparison of the data to the model predictions can be performed, the sensitivity of both T_B and $dN/dy^{(0)}$ to in-medium effects is quite small. A decisive test would be to extend the measurements to mid-rapidity where this sensitivity is most pronounced.

4.2. K^-/K^+ RATIO

In this section we investigate the rapidity and transverse momentum dependence of the K^-/K^+ ratio. This is motivated by the following considerations. According to Fig. 1, in-medium effects are much more important for K^- than for K^+. However the K^- production yield at SIS energies being very small, the limited statistics (Tab. 1) doesn't allow to examine the full K^- phase space distributions with a high accuracy. The study of the K^-/K^+ is meaningful and particularly interesting since by doing so statistical limitations and experimental detector inefficiencies cancel-out to some extent. In addition, since in-medium effects act oppositely on K^- and K^+ (Fig. 1), their ratio should be most sensitive to these effects. One has nevertheless to restrict the study to the fraction of phase space where the ratio can be defined, *i.e.* to the fraction of phase space in which K^- are identified since the latter is smaller than the one occupied by identified K^+.

Figure 4 show the K^-/K^+ ratio as a function of rapidity and transverse momentum. As it can be observed, the introduction of in-medium effects in the calculations leads to completely different distributions both in shape and magnitude. Without in-medium effects the ratio is found to decrease slightly from target/spectator rapidities to c.m. rapidity. This is understood as being due to absorption of slow moving K^- [29]. Oppositely, with in-medium effects, a well defined maximum appears at mid-rapidity. It can be interpretated as the consequence of the interplay of three effects : *i)* according to Fig. 1, the yield of K^- is enhanced more than the one of K^+ is reduced, *ii)* this is the most pronounced at mid-rapidity where, thanks to the high energy density, K^- are produced more abundantly, and *iii)* the effective K-nucleon potential tends to push K^+ away from nucleons (*i.e.* to large rapidities) and to attract K^- towards nucleons (*i.e.* to small rapidities). The latter effect is also well seen in the transverse momentum dependence of the ratio since, due to the K-nucleon potential, K^+ are pushed towards high momenta whereas K^- are pulled towards low momenta. The data are nicely reproduced by the calculations only if in-medium effects are taken into account. A further careful analysis has demonstrated that Coulomb interaction can't account for the observed experimental trends [30].

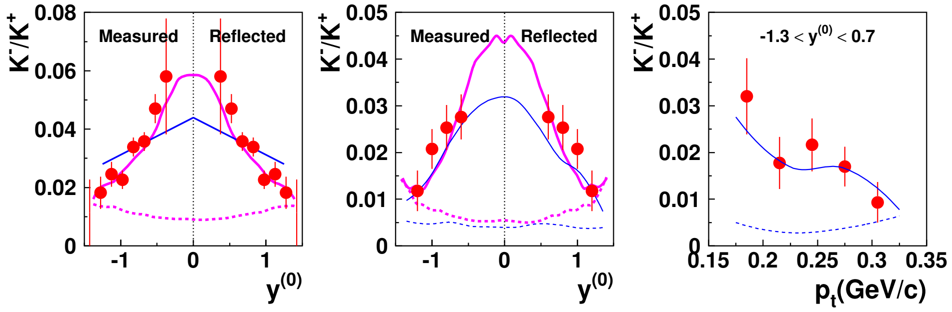

Figure 4. K^-/K^+ ratio as a function of *i)* rapidity in Ni + Ni reactions at 1.93 AGeV (left), *ii)* rapidity in Ru + Ru reactions at 1.69 AGeV (midle) and *iii)* transverse momentum in Ru + Ru reactions at 1.69 AGeV (right). The selected event classes correspond to a centrality of $b < 4$ fm. Data (dots) are compared to the prediction of RBUU models with (solid curves) and without in-medium effects (dashed curves). Thick (resp. thin) curves correspond to calculations from [29] (resp. [31]). Error bars represent statistical uncertainties. Adapted from [30,32].

5. Kaon sideward flow

Collective flow effects of various ejectiles emerging from a heavy ion reaction are of great interest since they are known as a sensitive probe of compression of nuclear matter [33]. These collective phenomena were predicted by nuclear hydrodynamical models [34] and experimentally identified in the eighties with the advent of the first generation of 4π detectors. Different forms of baryonic matter flow were observed : *i)* the directed sideward flow [35] which appears as a deflection of the emitted particles in the reaction plane[3] *ii)* the squeeze-out effect which manifests itself as an enhanced emission perpendicular to the reaction plane [36, 37], and *iii)* the so-called

[3]The reaction plane of a collision is defined by the beam axis and the impact parameter vector.

radial flow which has been more recently evidenced by the FOPI collaboration as an azimuthally symmetric expansion in highly central collisions [38]. In this section we investigate the sideward flow not of baryons but of produced strange particles namely K^+ and Λ which was recently predicted to be sensitive to their in-medium potential [15, 39, 40]. The reaction plane was experimentally reconstructed event wise, according to the method proposed in [41], with an accuracy of about 40° depending on beam energy, system size and centrality.

5.1. K^+ FLOW IN NI + NI AT 1.93 AGEV

Figure 5 shows the sideward-flow of K^+, proton, K^0_S and Λ measured in central Ni + Ni collisions at 1.93 AGeV [21, 42]. The results are presented in terms of the mean in-plane transverse momentum component divided by the particle mass as a function of the normalized rapidity $y^{(0)}$.

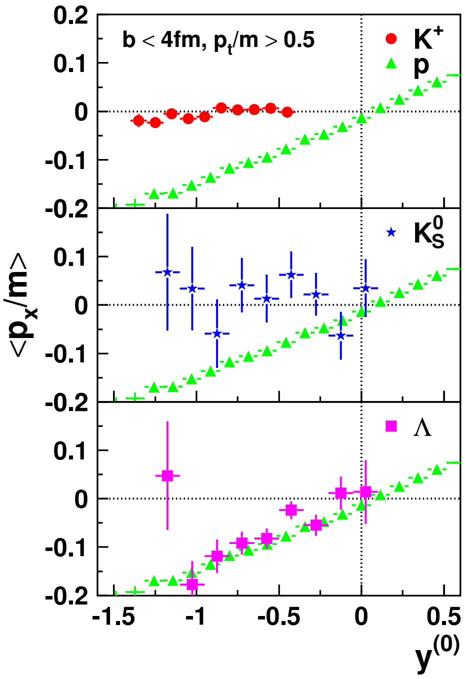

Figure 5. Sideward flow of K^+ (dots), protons (triangles), K^0_S (stars) and Λ (squares) in central ($b < 4$ fm) Ni + Ni collisions at 1.93 AGeV. Data for K^0_S and Λ (resp. K^+ and protons) are from [21] (resp. [42])

Protons exhibit the well-known shape characterizing an in-plane collective deflection. On the other hand, the flow pattern of produced particles shows a striking feature : although kaons and Λ are created under the same mechanisms during the reaction (associate production), Λ flow is very similar to the one of proton whereas kaons show a vanishing flow *i.e.* a signal compatible with zero. This difference can't be explained by short range correlations since the measured K-nucleon and Λ-nucleon interaction cross-sections being quite similar (of the order of 10-15 mb [43]), rescattering effects are found to play a comparable role on K^+ and Λ sideward-flow [40]. Classical long range correlations such as Coulomb potential can't neither be invoqued since one would then expect to observe a different flow pattern for charged and neutral kaons which is not the case within errors. One would have therefore to consider the existence of an additional "non-classical" repulsive K^+-nucleon potential. In order to achieve a meaningful interpretation of the experimental trends, the K^+ flow data were extensively compared to different model predictions in the two scenarios already described (with and without in-medium effects). Such comparisons are shown in Fig. 6.

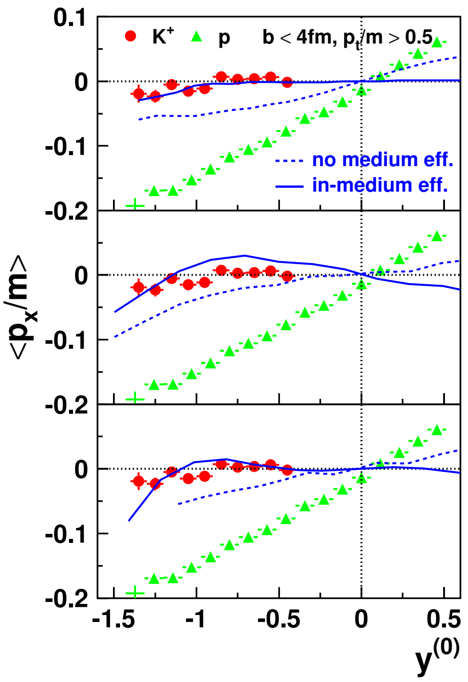

Figure 6. Sideward flow of K^+ (dots), protons (triangles), in central ($b < 4$ fm) Ni + Ni collisions at 1.93 AGeV. K^+ data (from [42]) are compared to the calculations from [44] (upper frame), [45] (midle frame) and [46] (lower frame) with in-medium effects (solid curves) and without in-medium effects (dashed curves).

Although the magnitude of the predicted effect is slightly different from one model to another, the experimental trend clearly supports an in-medium potential scenario for K^+ thus implying the existence of a repulsive K^+-nucleon mean field. However this statement has to be taken carefully since *i)* an alternative description of the data was proposed in [47] invoking rescattering effects instead of in-medium kaon potentials, *ii)* the sensitivity of K^+ sideward flow to in-medium effects was found in [48] to be washed-out when a momentum dependence of the potential is included in the calculations, and *iii)* it was recently pointed-out in [49] that the lifetime of nuclear resonances (Δ's) used in the models is partially responsible for the magnitude of the K^+ sideward flow as it is a crucial ingredient for kaon production channels.

5.2. K^+ FLOW IN RU + RU AT 1.69 AGEV

In order to further elucidate these questions, K^+ sideward flow in the Ru + Ru system at 1.69 AGeV has been investigated recently. Such a heavy system is well suited for flow studies since flow effects are larger as compared to lighter systems [4]. It allows in addition to study K^+ flow in non-central collisions where, due to a large sensitivity of the observable to in-medium effects, an anti-flow phenomenon is expected to be seen [31, 40] (Fig. 7).

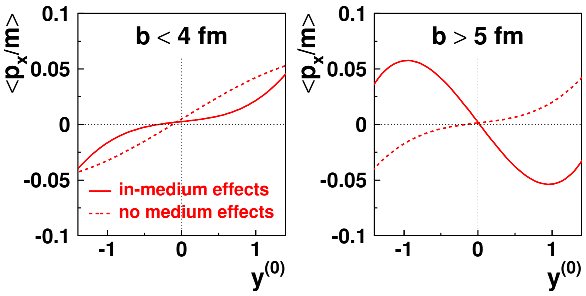

Figure 7. Model predictions [31] for K^+ flow in Ru + Ru collisions at 1.69 AGeV with (solid curves) and without (dashed curves) in-medium effects (b is the reaction impact parameter). Taken from [50].

Preliminary experimental results on the centrality dependence of the K^+ flow in Ru + Ru reactions at 1.69 AGeV are shown in Fig. 8.

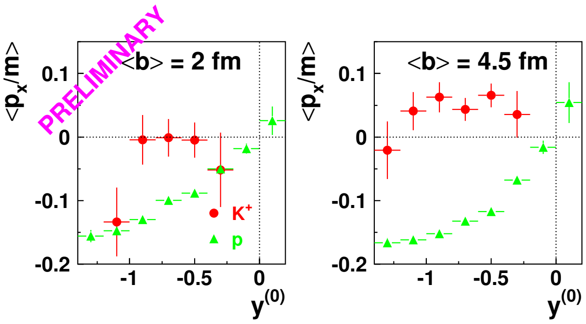

Figure 8. Flow of K^+ (dots) and protons (triangles) in central (left) and semi-central (right) Ru + Ru events at 1.69 AGeV. Error bars represent statistical uncertainties. Taken from [50].

The events were centrality selected by imposing cuts on the multiplicity of charged particles, PMUL, detected in the forward Plastic Wall of the FOPI detector. For the most central sample an additional condition on the global quantity ERAT [4] was applied. A clear change in the K^+ flow pattern can be observed from a close-to-vanishing signal in central collisions to an anti-flow in semi-central collisions. This trend is in qualitative agreement with the model predictions shown in Fig. 7 if in-medium modification of the K^+ properties are taken into account. Although the change in the K^+ flow pattern between central and semi-central collisions is obvious, a quantitative statement about the magnitude of the signal is difficult at the present status of the analysis. The latter was found to depend somewhat on the applied quality criteria for the tracks in the CDC and their matching with the Barrel. Further analysis is in progress.

6. Summary and outlooks

Kaon phase space distributions and flow have been investigated in Ni + Ni and Ru + Ru collisions between 1 and 2 AGeV with the FOPI detector. Data were compared to model predictions investigating in-medium modifications of kaon properties. The overall picture emerging from the comparison tends to favour the existence of in-medium effects on kaons. In particular, it was established that the experimental K^-/K^+ ratio as well as the K^+ flow can't be consistently described by "classical" transport model theories which do not include in-medium effects. To which extent these observations can be interpreted as a consequence of a partial restoration of chiral symmetry in the nuclear medium remains an open question since alternative descriptions of the data might be elaborated. In addition, before to draw any final statement on kaon data, one would have to carefully compare baryon data with the same transport model calculations.

Further exciting possibilities will be offered soon with the upgrade of the FOPI detector time-of-flight system. This will allow to study with better statistics and accuracy K^-'s for which in-medium effects are expected to be much more pronounced. In addition, the study with FOPI of the ϕ meson from its K^-K^+ decay channel combined together with the e^-e^+ decay channel measured with HADES at GSI will shine more light in this intriguing issue.

Acknowledgements

It is a pleasure to acknowledge the organizers of the workshop for their invitation and the members of the FOPI collaboration at GSI for several fruitful discussions.

The members of the FOPI collaboration are : J.P. Alard, A. Andronic, R. Averbeck, Z. Basrak, N. Bastid, I. Belyaev, A. Bendarag, G. Berek, D. Best, R. Čaplar, N. Cindro, P. Crochet, A. Devismes, P. Dupieux, M. Dželalija, M. Eskef, Z. Fodor, L. Fraysse, A. Genoux-Lubain, A. Gobbi, Y. Grishkin, N. Herrmann, K.D. Hildenbrand, B. Hong, J. Kecskemeti, Y.J. Kim, M. Kirejczyk, M. Korolija, R. Kotte, M. Kowalczyk, T. Kress, R. Kutsche, A. Lebedev, K.S. Lee, Y. Leifels, V. Manko, H. Merlitz, S. Mohren, D. Moisa, W. Neubert, A. Nianine, D. Pelte, M. Petrovici, C. Plettner, F. Rami, W. Reisdorf, B. de Schauenburg, D. Schüll, Z. Seres, B. Sikora, K.S. Sim, V. Simion, K. Siwek-Wilczyńska, A. Somov, M. Stockmeier, G. Stoicea, M. Vasiliev, P. Wagner, G.S. Wang, K. Wiśniewski, D. Wohlfarth, J.T. Yang, I. Yushmanov, A. Zhilin

References

1. R. Stock, *Phys. Rep.* **135 (1986) 261**
2. J. Aichelin, *Phys. Rep.* **202 (1991) 233**
3. H.H. Gutbrod *et al.*, *Rep. Prog. Phys.* **52 (1989) 1267**
4. W. Reisdorf and H.G. Ritter, *Ann. Rev. Nucl. Part. Sci.* **47 (1997)**
5. N. Herrmann, *Nucl. Phys.* **A 610 (1996) 49c**
6. R. Averbeck, *nucl-ex/9803001* **(1998)**
7. V. Metag, *GSI-Preprint* **98-09 (1998)**, proceedings of Quark Matter '97
8. C.M. Ko and G.Q. Li, *J. Phys.* **G 22 (1996) 1673**
9. C.M. Ko *et al.*, *Ann. Rev. Nucl. Part. Sci.* **47 (1997)**
10. G.Q. Li *et al.*, *Nucl. Phys.* **A 611 (1996) 539**
11. A. Drees, *Nucl. Phys.* **A 610 (1996) 536c**
12. J. Rafelski and B. Müller, *Phys. Rev. Lett.* **48 (1982) 1066**
13. G.E. Brown *et al.*, *Phys. Rev.* **D 37 (1988) 2042**
14. D.B. Kaplan and A.E. Nelson, *Phys. Lett.* **B 174 (1986) 57**; A.E. Nelson and D.B. Kaplan, *Phys. Lett.* **B 192 (1987) 193**
15. G.Q. Li, *et al.*, *Phys. Rev. Lett.* **74 (1995) 235**
16. G.Q. Li *et al.*, *Nucl. Phys.* **A 625 (1997) 372**
17. C.H. Lee, *Phys. Rep.* **275 (1996) 255**
18. T.Waas *et al.*, *Phys. Lett.* **B 379 (1996) 34**
19. J. Schaffner *et al.*, *Phys. Lett.* **B 334 (1994) 268**
20. W.Cassing *et al.*, *Nucl. Phys.* **A 614 (1997) 415**
21. J. Ritmann and the FOPI collaboration, *Z. Phys.* **A 352 (1995) 355**
22. R. Barth *et al.*, *Phys. Rev. Lett.* **78 (1997) 4007**
23. A. Gobbi and the FOPI Collaboration, *Nucl. Inst. Meth.* **A 324 (1993) 156**
24. B. Hong and the FOPI collaboration, *Phys. Lett.* **B 407 (1997) 115**
25. B. Hong and the FOPI collaboration, *Phys. Rev.* **C 57 (1998) 244**
26. D. Best and the FOPI collaboration, *Nucl. Phys.* **A 622 (1997) 573**
27. K. Wiśniewski, *PhD Thesis, University of Warsaw, Poland*
28. W. Cassing and U. Mosel, *Prog. Part. Nucl. Phys.* **25 (1990) 235**
29. G.Q. Li and G.E. Brown, *nucl-th/9804013* **(1998)**
30. K. Wiśniewski and the FOPI collaboration, *to be published*
31. E.L. Bratkovskaya and W. Cassing, *private communication*
32. K. Wiśniewski and the FOPI collaboration, *GSI Annual Report* **(1997) 60**
33. H. Stöcker *et al*, *Phys. Rev. Lett.* **44 (1980) 725**
34. W. Scheid *et al.*, *Phys. Rev. Lett.* **32 (1974) 741**
35. H.A. Gustafsson *et al.*, *Phys. Rev. Lett.* **52 (1984) 1590**
36. H.H. Gutbrod *et al.*, *Phys. Lett.* **B 216 (1989) 267**
37. M. Demoulins *et al.*, *Phys. Lett.* **B 241 (1990) 476**
38. S.G. Jeong and the FOPI Collaboration, *Phys. Rev. Lett.* **72 (1994) 3468**
39. G.Q. Li and C.M. Ko, *Nucl. Phys* **A 594 (1995) 460**; G.Q. Li and C.M. Ko, *Phys. Rev.* **C 54 (1996) R 2159**; G.Q. Li *et al.*, *Phys. Lett.* **B 381 (1996) 17**
40. G.Q. Li and G.E. Brown, *nucl-th/9804018* **(1998)**
41. P. Danielewicz et al., *Phys. Lett.* **B 157 (1985) 146**
42. J. Ritmann and the FOPI collaboration, *GSI Annual Report* **(1996) 61**
43. A. Baldini *et al.*, *Total Cross Sections for Reactions of High Energy Particles*, **Springer-Verlag, Heidelberg (1988)**
44. G.Q. Li et al., *nucl-th/9703040* **(1997)**
45. E.L. Bratkovskaya et al., *Nucl. Phys.* **A 622 (1997) 593**
46. Z.S. Wang et al., *nucl-th/9706047* **(1997)**
47. C. David *et al.*, *nucl-th/9611016* **(1996)**
48. C. Fuchs *et al.*, *nucl-th/9801048* **(1998)** to appear in *Phys. Rev. Lett.*
49. C. David *et al.*, *nucl-th/9805017* **(1998)**
50. P. Crochet and the FOPI collaboration, *GSI Annual Report* **(1997) 59**